Subharmonic Resonance in a Mixing Layer

By N. N. Mansour [1], F. Hussain [2], and J. C. Buell[1]

The subharmonic resonance phenomenon in a spatially-evolving mixing layer is studied using direct simulations of the two-dimensional Navier-Stokes equations. The computational domain extends to $\pm\infty$ in the cross-stream direction with $U_1 = 1.25$ and $U_2 = 0.25$ imposed at $+\infty$ and $-\infty$ respectively. The domain is finite in the streamwise direction with inflow and outflow boundary conditions imposed at $x/\delta_w = 0$ and $x/\delta_w = 100$, respectively. A hyperbolic-tangent mean velocity profile is assumed at the inlet and the Reynolds number based on the inlet vorticity thickness and velocity difference is $Re = 600$. It is observed that the phase angle between the fundamental and its subharmonic plays a key role in the spatial development of these modes. Contour plots of vorticity show that varying the phase will have a dramatic effect on the dynamics of the vortices. Pairing or shredding is observed depending on the phase. Fourier decomposition of the time traces show that the fundamental grows, saturates and decays with the downstream distance. The subharmonic has a similar behavior. However, the level at which the modes will saturate is affected by the phase. At 0° phase, we find that as the fundamental saturates, the growth rate of the subharmonic is enhanced. At 90° phase, we find that as the fundamental saturates, the growth rate of the subharmonic is inhibited. In the later case, the growth rate of the subharmonic recovers after saturation of the fundamental. These results are in qualitative agreement with experimental data.

1. Introduction

While the occurrence of large-scale, vortical coherent structures (CS) in turbulent shear flows is not in question, what role they play, how this role is affected by the interaction of these CS and how this role can be enhanced or suppressed through manipulation of CS are still open questions. The initiation, growth, interaction, breakdown and regeneration of coherent structures are manifestations of a hierarchy of instability mechanisms in both transitional and turbulent flows. In a turbulent flow the interaction of coherent structures is complex and three-dimensional. The interaction of 2D coherent structures in a mixing layer should be addressed first as the simpler case. Following the 2D roll-up of an initially laminar layer into discrete structures, the most common, and dynamically significant, event observed is the growth of the subharmonic which manifests itself as pairings. The pairing process, i.e., the growth of the subharmonic, is a consequence of what has come to be known as *subharmonic resonance* - a simple consequence of nonlinear interaction between a

1 NASA Ames Research Center
2 University of Houston

wave of angular-frequency ω and its subharmonic wave (of angular-frequency $\omega/2$). Under suitable conditions (say proper choices of relative phase and amplitudes of ω and $\omega/2$ components) the fundamental component that results from nonlinear interaction can reinforce the subharmonic. The resulting growth of the subharmonic, causing merger of the vortices, is one of the most striking features of turbulent shear flows because it provides a direct mechanism for large-scale mixing and other phenomena such as aerodynamic noise.

The subharmonic resonance mechanism was first analyzed by Kelly (1967) using a weakly nonlinear temporal formulation for a parallel flow. He showed that the mean together with a fundamental wave component can reinforce the growth of the subharmonic of that fundamental. Monkewitz (1988) extended Kelly's analysis to spatially evolving mixing layers and addressed some interesting features: effect of the phase angle between the fundamental and subharmonic, the critical fundamental amplitude required for resonance and the effect of detuning. The phenomenon has been studied numerically by Patnaik et al. (1976) and Riley & Metcalfe (1980) for the time-developing mixing layer. In this work the spatial mixing layer is investigated.

The computational scheme uses high-order approximations to the two-dimensional Navier-Stokes equations. A spatially evolving mixing layer is studied by forcing the inlet flow with the eigenfunction solutions to the Rayleigh equation at the desired frequencies. The boundary conditions used are described in section 2. Vorticity contours, time spectra and the spatial development of the modes are discussed in section 3.

2. The computational parameters

The numerical scheme approximates the Navier-Stokes equations by using a spectral method in the vertical direction, high-order Padé finite differencing in the streamwise direction and third-order Runge-Kutta in time. The mean inlet streamwise velocity is forced to be a tanh profile,

$$U_{inlet} = \frac{1}{2} \left(\frac{1+r}{1-r} + \tanh(2y) \right) \tag{1}$$

where $r = U_1/U_2$ is the velocity ratio of the low-speed side over the high-speed side. All lengths are nondimensionalized with the vorticity thickness, δ_w, of the inlet mean flow, all velocities are nondimensionalized with the velocity difference, $\Delta U = U_1 - U_2$. To correspond with the experiment of Husain & Hussain (1986) we want $r = 0$; however, computationally the exit boundary conditions for this case are harder to prescribe. At the exit the structures are assumed to convect out of the domain at a constant convection speed (c),

$$\frac{\partial}{\partial t} u_i + c \frac{\partial}{\partial x} u_i = 0$$

for both the streamwise and cross-stream velocity. If the velocity at the low speed side is too low there will be intermittent backflow at the exit boundary which

Case	α_1	α_2	ϕ	Summary
1	0.005	0.	0°	Forcing only the fundamental.
2	0.	0.005	0°	Forcing only the subharmonic.
3	0.005	0.005	0°	Forcing both the fund. and its sub. with 0° phase.
4	0.005	0.005	90°	Forcing both the fund. and its sub. with 90° phase.

Table 1. Summary of computed cases

will violate our "convection out of the domain" assumption. We chose $r = 0.2$. Proper prescription of the exit boundary condition is still an unsolved problem. Buell & Huerre (this proceeding) found that the exit boundary condition causes global potential fluctuations which interact with the inflow boundary and create small-amplitude noise at the inlet. In our study we will force the inlet flow at one frequency and its subharmonic. The amplitude of the forcing (0.005 of the velocity difference) is much larger than the feedback amplitude. It is found that the growth rate of the forced frequency is not affected by the boundary feedback problem.

The boundary condition at $\pm\infty$ is imposed so that the streamwise velocity is constant and equal to $U_1 = 1.25$ and $U_2 = 0.25$ at $+\infty$ and $-\infty$ respectively. The cross stream velocity can be defined arbitrarily at these boundaries. Numerical experimentation with $r = 0.2$ suggest the values $V_1 = -0.002$ and $V_2 = 0.005$ at $+\infty$ and $-\infty$ respectively. These entrainment velocities were selected to minimize the streamwise pressure gradient. Numerical experimentation with these boundary conditions show that the level of the cross-stream velocity will not affect the vorticity thickness of the layer but has a direct effect on the momentum thickness.

The inlet profile is forced as follows:

$$
\begin{aligned}
u_1 &= U_{inlet} + \alpha_1 \text{Real}(\hat{u}_f \exp(-i\omega t)) + \alpha_2 \text{Real}(\hat{u}_{f/2} \exp(-i(\omega t/2 + \phi))) \\
u_2 &= \alpha_1 \text{Real}(\hat{v}_f \exp(-i\omega t)) + \alpha_2 \text{Real}(\hat{v}_{f/2} \exp(-i(\omega t/2 + \phi)))
\end{aligned}
\tag{2}
$$

where ω is a fundamental frequency, $\hat{u}_f$, $\hat{v}_f$, ..., are the eigenfunctions of the Rayleigh equation corresponding to the forced frequencies, and ϕ is the phase difference between the fundamental and its subharmonic. α_1 and α_2 are arbitrary constants that were set equal to $\alpha_1 = \alpha_2 = 0.005$.

3. Basic measured quantities

Numerical integration of the Rayleigh equation show that the most unstable angular frequency is about $\omega = 0.65$ for the mean profile given by Eq. (1). We will choose this frequency as our fundamental frequency. The objective of this work is to study the effect of the phase difference between the fundamental and its subharmonic on the development of the layer. We know that mixing layers develop by the interaction of vortices and that the layer grows by the amalgamation of these vortices.

3.1 Vorticity Contours

Figures 1a-d show characteristic vorticity contours after the layer has developed for the four cases that are summarized in Table 1. Case 1 corresponds to forcing the fundamental without forcing the subharmonic. Case 2 corresponds to the case
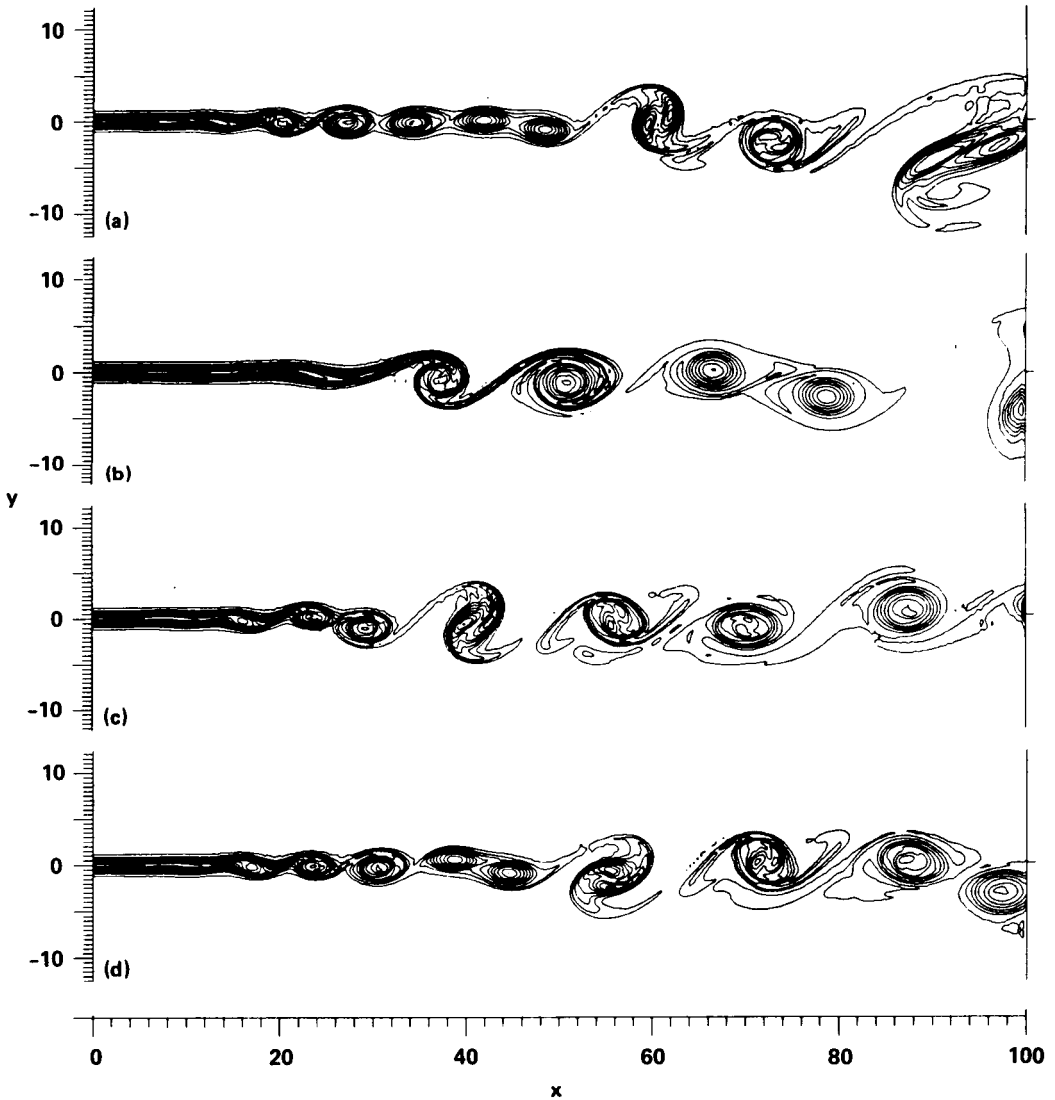
FIGURE 1.   Contour plots of vorticity. a) Case 1, forcing the fundamental only. b) Case 2, forcing the subharmonic only. c) Case 3, forcing the fundamental and its subharmonic with $\phi = 0°$. d) Case 4, forcing the fundamental and its subharmonic with $\phi = 90°$.

where only the subharmonic is forced. In case 3 both the fundamental and the subharmonic are forced with $\phi = 0°$ phase difference between them. In case 4 the fundamental and subharmonic are forced with $\phi = 90°$ phase difference between them. One can notice that in all cases the layer breaks into vortices corresponding
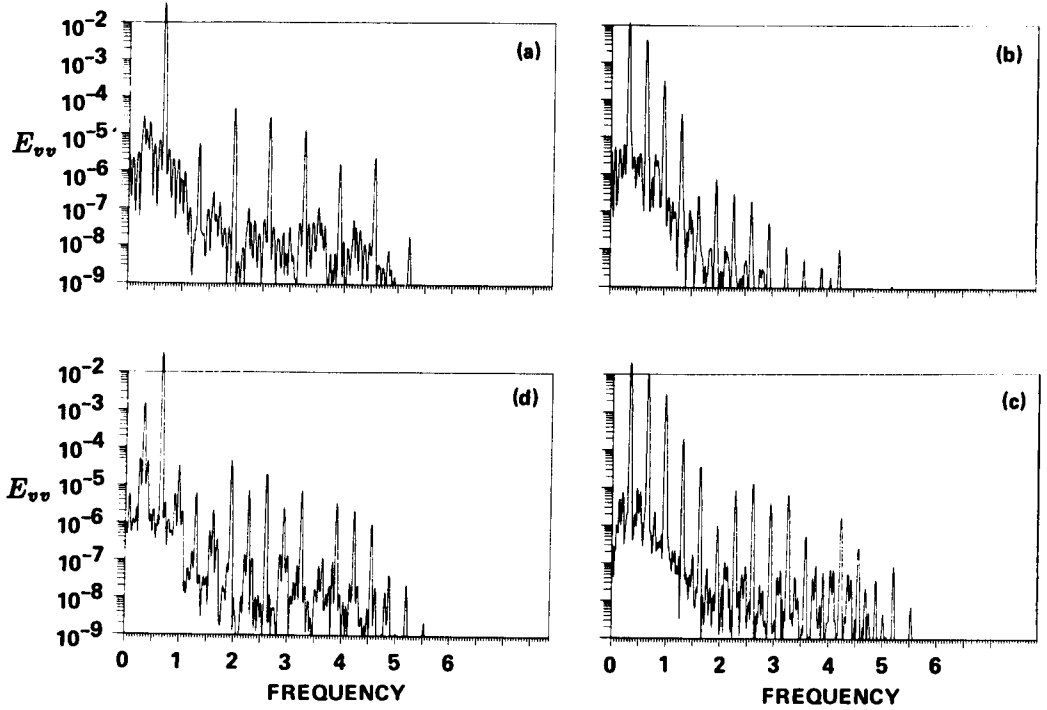
FIGURE 2. Time spectra at $x = 28.1$ and $y = 0$. a) Case 1, forcing the fundamental only. b) Case 2, forcing the subharmonic only. c) Case 3, forcing the fundamental and its subharmonic with $\phi = 0°$. d) Case 4, forcing the fundamental and its subharmonic with $\phi = 90°$.

to the forced frequency. These vortices subsequently pair. The growth of the subharmonic (pairing of the forced frequency) that occurs in case 1 is due to the effect of the downstream boundary condition on the layer. In our reference frame the mixing layer should be convectively unstable, therefore, no subharmonic can be generated unless it is forced from the upstream. Because the inlet for cases 1 and 2 is forced at one frequency only, the appearance of the subharmonic as detected by the pairing can only come from the effect of the downstream boundary condition on the upstream. Comparing the four cases, we find that the earliest pairing occurs in case 3 where the subharmonic was forced with $\phi = 0°$.

The layer is thicker (at $x = 40$) for this case as compared to the other cases. By changing the phase to 90° the location of the pairing is shifted downstream. Comparing the case of $\phi = 90°$ phase difference (Figure 1d) with the case of forcing only the fundamental (Figure 1a), we find that the two layers are similar. This is an indication that the subharmonic is being inhibited for $\phi = 90°$. The suppression is not complete since pairing in case 4 still occurs earlier than in case 1.

Vorticity contours yield a qualitative picture on the development of the layer. A series of contour plots as a sequence in time or a movie will yield a better picture of the dynamics of the layer, but the information they will yield is still qualitative.

3.2 Time spectra

An effective tool for the study of unsteady data is to analyze the time signal using Fourier transforms in time. Given the time trace of the velocity component at a location in space, the signal is windowed, and then expanded in a Fourier series in time,

$$v = \sum_{\omega} \hat{v}(\omega) \exp(i\omega t)$$

The spectrum of the velocity is defined as,

$$E_{vv}(\omega) = \hat{v}(\omega)\hat{v}^*(\omega).$$

Figures 2a and 2b show the spectra of the v-velocity component at $x = 28.1$, and $y = 0$ for the four cases. We can see clearly that modes other than the forced modes and their harmonics have developed. The development of a broad spectrum is due to the interaction of the downstream boundary condition with the inlet flow. This interaction is forcing a background noise which is unavoidable in experiments. Since we are forcing a given frequency and are interested in the early development of the layer, we expect that the effect of the downstream boundary condition on our results and conclusion should be small. This is supported by the fact that the forced frequencies and their harmonics are still the dominant frequencies at $x < 30$. Comparison of Figures 2c and 2d show that the subharmonic is much larger for case 3 as compared to case 2. This is an indication that the growth rate of the subharmonic is larger for $\phi = 0°$. Comparing the amplitude of the fundamental for the three cases (1, 3 and 4), we find that the magnitude of the fundamental is comparable for cases 1 and 4; for case 3, the growth of the subharmonic has inhibited the fundamental. In case 2, the fundamental is a harmonic of the forced frequency and is expected to be lower than the forced cases. To properly compare the growth rate of the different modes we need to examine the development of the modes in space.

3.3 Contour plots of Fourier modes.

In our discussion on the development of the layer (§3.1) we implicitly decomposed the flow field into its Fourier components. In the present study we are interested in the spatial distribution of the forced modes. Figures 3 and 4 show contour plots of $|\hat{u}_{f/2}|$ and $|\hat{v}_{f/2}|$ for cases 3 and 4. From these figures we find that $|\hat{u}_{f/2}|$ will grow in the downstream direction and develop a double peak. Contour plots of $|\hat{v}_{f/2}|$ (see Figure 3) show that in the early stages $|\hat{v}_{f/2}|$ has one peak close to the centerline. The effect of the phase difference is manifested by the shift in the downstream direction of the peak. For case 3, the subharmonic saturates at around $x = 40$, while for case 4 the peak occurs at around $x = 50$. Comparing the contour plots for the two cases, we find general similarities. Both $|\hat{u}_{f/2}|$ contours exhibit a region
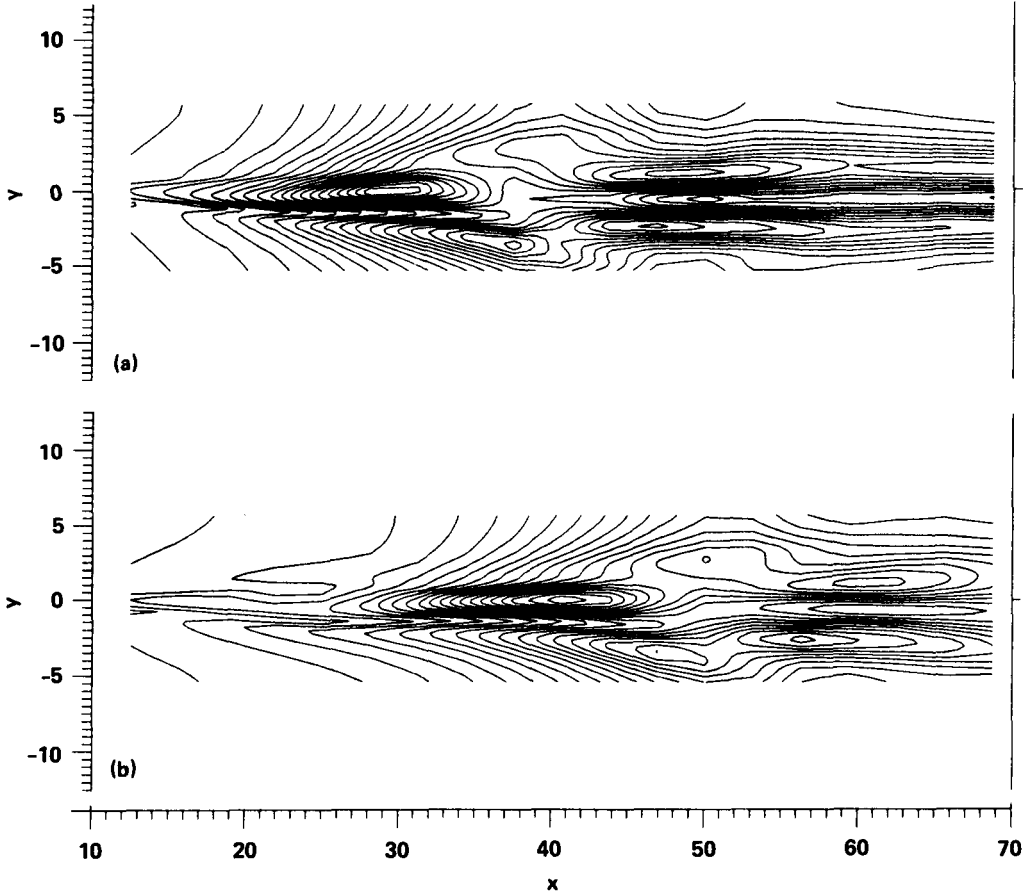
FIGURE 3. Contour plots of $|\hat{u}_{f/2}|$. a) Case 3, forcing the fundamental and its subharmonic with $\phi = 0°$. b) Case 4, forcing the fundamental and its subharmonic with $\phi = 90°$.

with double peaks, then a region of decay, followed again by a region with double peaks. Quantifying the $|\hat{u}_{f/2}|$ by plots of the intensity at one y location will not yield a proper norm since this component varies rapidly across the layer.

In general, the $|\hat{v}|$ component is simpler to quantify . Contour plots of $|\hat{v}|$ show a peak around $y = 0$ for both cases. The two plots are similar; however, shifting the coordinate so that the peaks will coincide shows that the distribution of the modes in space is different. The distance between contour levels in case 3 is shorter, indicating that the subharmonic is growing at a faster rate.

3.4 Growth of the fundamental and Subharmonic

While contour plots show the distribution of the mode in space, it is not simple to compare the data for the different cases. For simplicity, we assume that a proper
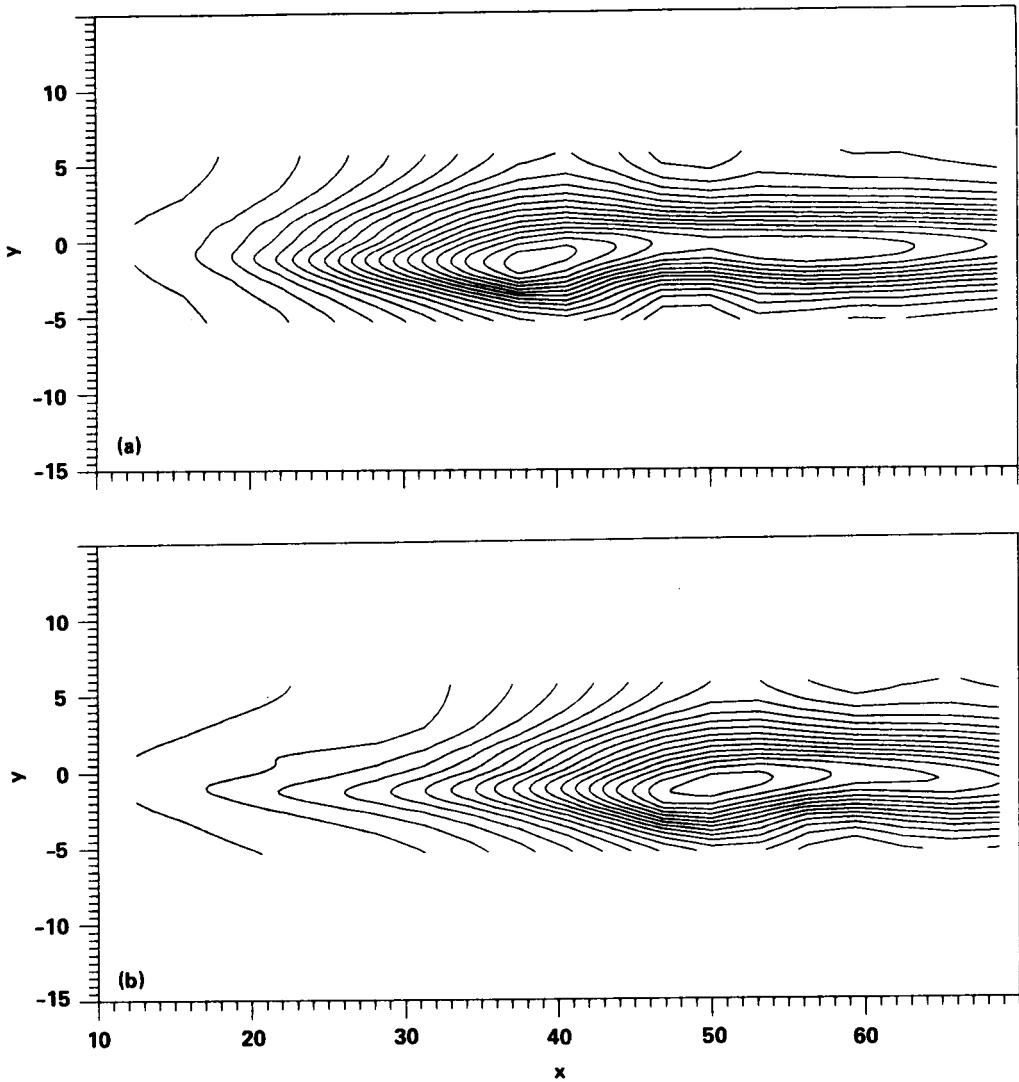
FIGURE 4.   Contour plots of $|\hat{v}_{f/2}|$. a) Case 3, forcing the fundamental and its subharmonic with $\phi = 0°$. b) Case 4, forcing the fundamental and its subharmonic with $\phi = 90°$.

norm for the distribution is well represented by the development of $|\hat{v}|$ along $y = 0$, and study the development of the fundamental and subharmonic along that line.

3.4.1 Effect of the Reynolds number.

At the early stages of the development of the modes and at high Reynolds numbers we expect linear theory to be a good approximation. At low Reynolds numbers the viscous growth of the layer will be important and will affect the growth rate of the
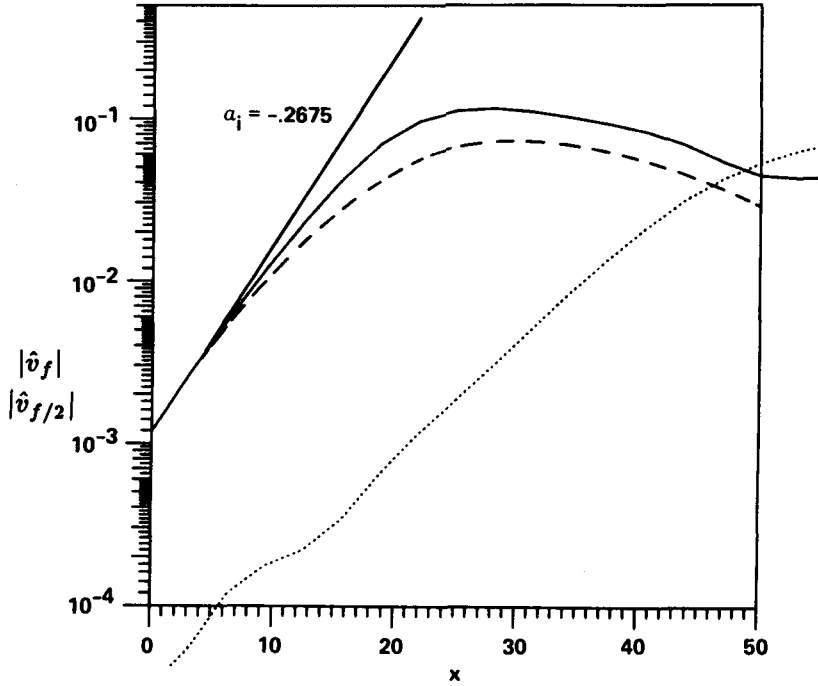
FIGURE 5. Effect of the Reynolds number on the development of the fundamental.
——— $|\hat{v}_f|$ with $Re = 600$. ---- $|\hat{v}_f|$ with $Re = 300$. ······· $|\hat{v}_{f/2}|$ with $Re = 600$.

modes. Figures 5 and 6 compare the development of $\hat{v}_f$ at $Re = 300$ and $Re = 600$ for cases 1 and 2 where only the fundamental and only the subharmonic is forced. We find that the effect of the Reynolds number is to reduce the growth rate in the downstream direction. This effect is less severe for the subharmonic mode. In addition, exponential growth is valid for significantly larger amplitudes of the subharmonic mode as compared to the fundamental mode. Note that in the case of forcing at only the fundamental, the subharmonic will develop because of feedback from the downstream boundary condition.

3.4.2 Effect of the phase difference on $|\hat{v}|$.

The development of the magnitude of the fundamental and its subharmonic with the downstream distance is shown in Figures 7a and 7b for $\phi = 0°$ and $\phi = 90°$ respectively. We find that the growth rate of the fundamental is only slightly affected by the presence of the subharmonic. However, the saturation level is higher for $\phi = 90°$ as compared to $\phi = 0°$. This is an indication that there is an interaction between the fundamental and its subharmonic. On the other hand the level at
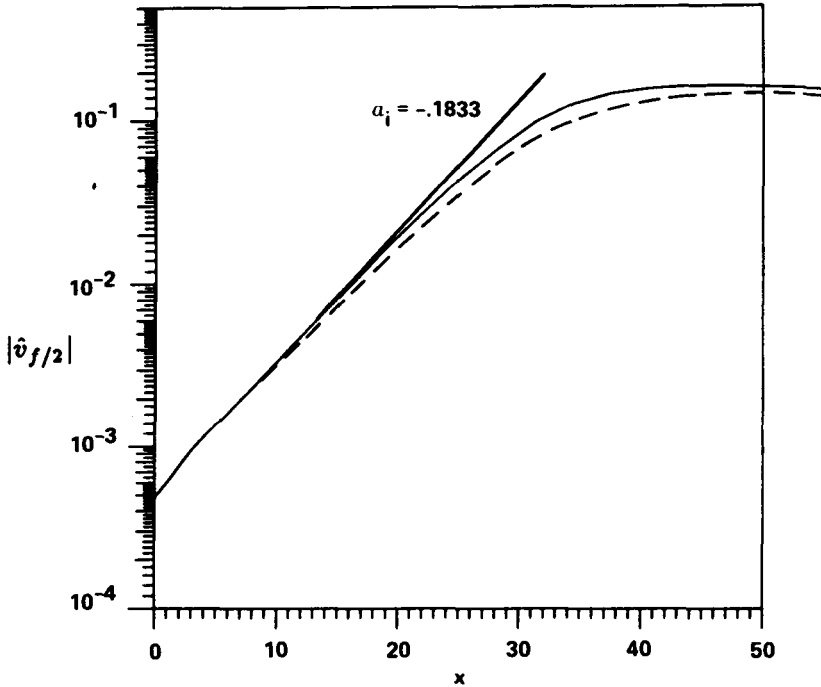
FIGURE 6. Effect of the Reynolds number on the development of the subharmonic.
——— $|\hat{v}_{f/2}|$ with $Re = 600$. - - - - $|\hat{v}_{f/2}|$ with $Re = 300$.

which the subharmonic saturates seems independent of the phase angle. But the location of the peak is dramatically affected by the phase angle. Comparison of the growth rate of the subharmonic with linear theory and case 2 (forcing only the subharmonic) shows that with $\phi = 0°$ the subharmonic grows faster than predicted by linear theory. On the other hand for $\phi = 90°$ its growth rate is suppressed as the fundamental saturates. After saturation the subharmonic recovers and starts growing. This is a clear indication that the phase between the fundamental and the subharmonic plays a critical role on the development of the layer. In agreement with Monkewitz's analysis we find that the amplitude of the fundamental has to reach a critical level before it can modify the growth rate of the subharmonic.

3.4.3 Effect of the phase difference on $|\hat{u}|$.

The effect of the phase difference on $|\hat{u}|$ is more dramatic that the effect on $|\hat{v}|$. Figures 8a and b show the development of $|\hat{u}_f|$ and $|\hat{u}_{f/2}|$ with the downstream direction at $y = 0$. We find that at $\phi = 90°$, $|\hat{u}_{f/2}|$ actually decreases as the fundamental saturates. After saturation the subharmonic grows at a faster rate than
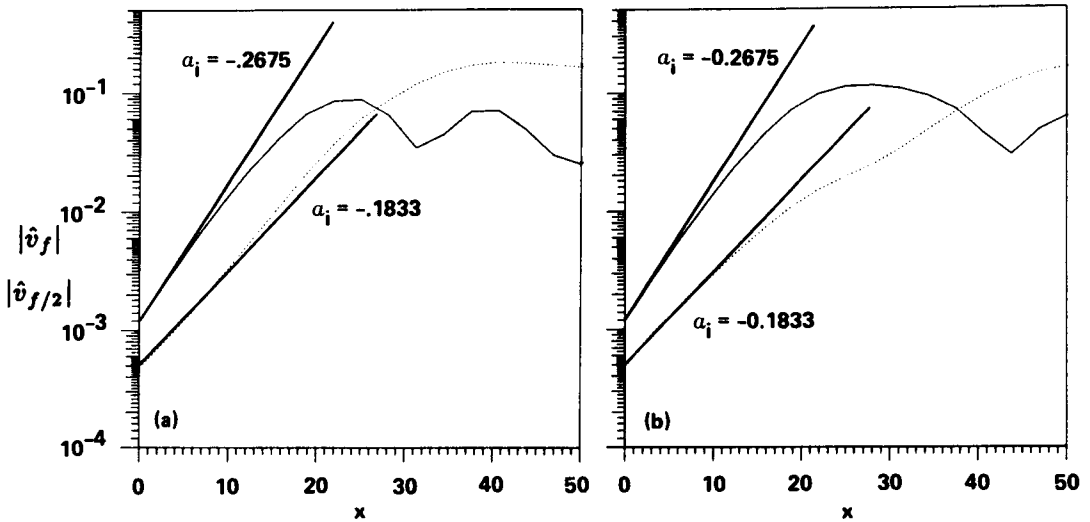
FIGURE 7. Development of $|\hat{v}_f|$ and $|\hat{v}_{f/2}|$ in the downstream direction at $y = 0$. a) Case 3, forcing the fundamental and its subharmonic with $\phi = 0°$. b) Case 4, forcing the fundamental and its subharmonic with $\phi = 90°$. ——— $|\hat{v}_f|$. ········ $|\hat{v}_{f/2}|$.

expected from linear theory. These observations are in qualitative agreement with the experimental measurements of Husain & Hussain (1986), but give a different pictures than Figure 7 on the development of the modes after saturation of the fundamental. This is an indication that results based on one component of the velocity should be interpreted with caution.

4. Future extensions

We have studied the effect of the phase angle between a fundamental and its subharmonic for one frequency, namely the most unstable frequency as predicted from linear theory. Two phases 90° apart were considered. In future work, the phase range $0° \leq \phi \leq 180°$ will be investigated. Early results indicate that the maximum suppression occurs at $\phi = 97°$. Also, in agreement with experimental observation, the maximum suppression occurs in a narrow phase range. This is an indication that suppression of mixing may be difficult to achieve in practical applications. Simulations at various frequencies will also be carried out to investigate the effect of Strouhal number on the phase difference between maximum enhancement and suppression. Finally, evaluation of different nonlinear theories on subharmonic resonance will be carried out by comparing the numerical results with the theoretical predictions and by evaluating the assumptions made by the theories.
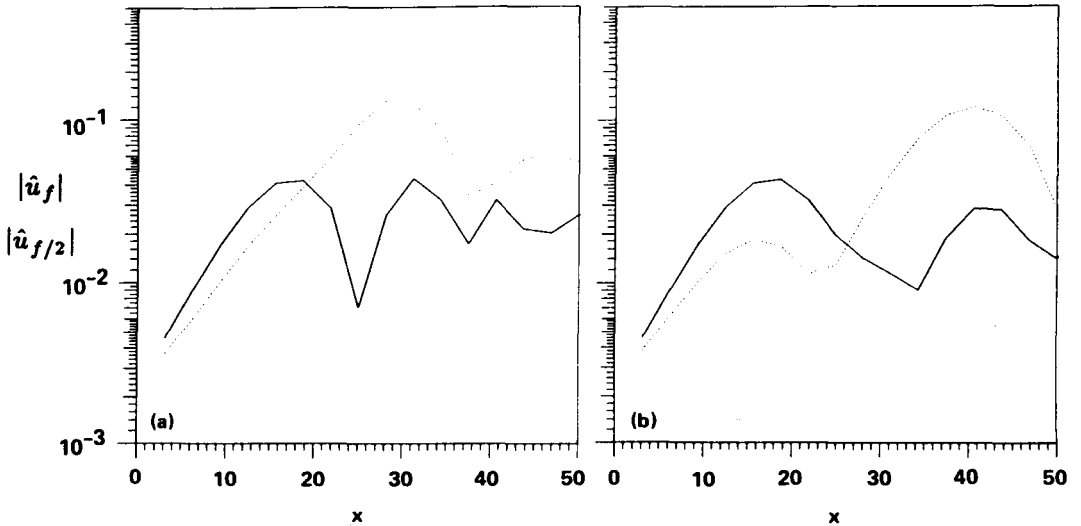
FIGURE 8.   Development of $|\hat{u}_f|$ and $|\hat{u}_{f/2}|$ in the downstream direction at $y = 0$. a) Case 3, forcing the fundamental and its subharmonic with $\phi = 0°$. b) Case 4, forcing the fundamental and its subharmonic with $\phi = 90°$. ———— $|\hat{u}_f|$. ········ $|\hat{u}_{f/2}|$.

REFERENCES

BUELL, J. C., AND HUERRE, P. 1988 . *Proceedings of the Summer Program 1988, Center for Turbulence Research, Ames Research Center.*

HUSAIN, H. S., AND HUSSAIN, F. 1986 . *Bull. of the Am. Phys. Soc.* **31**, 1696.

KELLY, R. E. 1967 . *J. Fluid Mech.* **27**, 657-689.

MONKEWETIZ, P. A. 1988 . *J. Fluid Mech.* **188**, 223-252.

PATNAIK, P. C., SHERMAN, F. S., AND CORCOS, G. M. 1976 . *J. Fluid Mech.* **73**, 215-240.

RILEY, J. J., AND METCALFE, R. W. 1980 . *AIAA paper 80-0274, Reno.*